

Jan Dutkiewicz<sup>1\*</sup>, Agata Kukuła-Kurzyniec<sup>1</sup>, Lidia Lityńska-Dobrzyńska<sup>1</sup>, Patrick Ochin<sup>2</sup>

<sup>1</sup> Institute of Metallurgy and Materials Science, PAS, ul. Reymonta 25, 30-059 Krakow, Poland

<sup>2</sup> CMPE Institut de Chimie et des Matériaux Paris Est CNRS-Université Paris-Est2-8 rue Henri Dunant F-94320 Thiais, France

\*Corresponding author: E-mail: nmdutkie@imim-pan.krakow.pl

Otrzymano (Received) 09.02.2012

## THE STRUCTURE AND PROPERTIES OF COMPOSITES BASED ON SILVER AND ALUMINIUM ALLOYS STRENGTHENED WITH AMORPHOUS PHASE

Silver base composites intended for electric contact materials with additions of 20% of amorphous phases based on zirconium or nickel good glass formers were consolidated from ball-milled powders. The structure was investigated using X-ray diffraction and TEM. The consolidated samples show an increase in hardness with an amorphous phase addition which is of the order of 100 HV for 20% of the amorphous phase. SEM and TEM structure studies have shown a nanocrystalline grain size in silver after milling and nanocrystalline intermetallic inclusions in the amorphous phase after hot pressing. DSC studies have shown a crystallization peak, confirming amorphization of the powders. The composites have shown a similar loss of mass during 50 000 contact operations, like conventional Ag-W composites. Another type of additions used to form aluminum alloy base nanocomposites was the amorphous powder of the alloy Al10%Ni10%Ti10%Zr (in at.%). Almost complete amorphization was observed after 60 hours of milling. TEM investigations allowed us to identify nanocrystalline intermetallic phases in the milled powders. The microhardness of the powder was very high - near 500 HV. Similar to the other types of composites, some growth of aluminum solid solution grains was observed and only a slight increase in the size of intermetallic phases was noticed. The compression strength was slightly lower than for aluminum alloy based ceramic composites due to crack formation in the amorphous phase.

**Keywords:** amorphous/crystalline composites, mechanical alloying, powder hot pressing, TEM

## STRUKTURA I WŁASNOŚCI KOMPOZYTÓW NA OSNOWIE SREBRA ORAZ STOPÓW ALUMINIUM WZMACNIANYCH FAZĄ AMORFICZNĄ

Kompozyty na osnowie srebra do zastosowań na kontakty elektryczne wykonano drogą metalurgii proszków poprzez prasowanie na gorąco w próżni. Jako dodatki umacniające do nanokrystalicznego proszku srebra stosowano dodatek amorficznego proszku ze stopów o dużej skłonności do tworzenia szkła na osnowie cyrkonu lub niklu uzyskanych przez mielenie w młynkach kulowych. Twardość kompozytów wzrasta wraz z zawartością fazy amorficznej, które osiągają twardość 100 HV dla 20% fazy amorficznej. Badania strukturalne metodami TEM i SEM wykazały rozdrobnienie ziarna srebra w mielonym proszku, a ponadto w kompozytach z dodatkiem fazy amorficznej obserwowano manometryczne wydzielania faz międzymetalicznych wewnątrz fazy amorficznej. Badania DSC wykazały krystalizację mielonych proszków amorficznych. Badania utraty masy podczas 50 000 cykli włączeniowych wykazały podobne właściwości jak konwencjonalnych materiałów Ag-W. Drugi badany rodzaj kompozytów z dodatkiem 34% wag. nanokrystalicznego stopu aluminium 7575 był również umacniany fazą amorficzną Al10%Ni10%Ti10%Zr (w % at.), uzyskaną poprzez mielenie w młynkach kulowych. Mikrotwardość frakcji amorficznej wynosiła 500 HV. Badania TEM kompozytów pozwoliły na identyfikację nanokrystalitów faz międzymetalicznych w osnowie amorficznej i pewien wzrost wielkości ziarna w stopie 7475. Uzyskano niższą wytrzymałość w próbie ściskania niż dla kompozytów na osnowie Al z dodatkiem fazy ceramicznej z uwagi na inicjację pęknięć w fazie amorficznej.

**Słowa kluczowe:** kompozyty amorficzno-krystaliczne, mechaniczna synteza, prasowanie proszków na gorąco, transmisyjna mikroskopia elektronowa

## INTRODUCTION

Amorphous particles or ribbons are being recently often applied as a strengthening phase of composites [1-13]. The most popular are amorphous-crystalline composites prepared using powder metallurgy or hot deformation joining methods with crystalline copper [2-5], nickel [2, 6, 7] or silver [13] additions which were intended to improve plasticity. Very good properties were obtained with a composite using a copper

base amorphous alloy with tantalum additions [1], where a compression strength above 2 GPa was obtained with good plasticity. The additions of 10% of copper or nickel acted in a similar way by slightly improving plasticity [2], with a similar strength as that of the amorphous near 2 GPa. Augmentation of copper content up to 40% in the amorphous matrix of spark plasma sintered samples caused a decrease in the

strength of composites to below 700 MPa [4]. The powders covered with nickel and spark plasma sintered [6,7] have shown very good plasticity and a compression strength better than that of pure amorphous spark plasma sintered samples, however, at a rather low strength - near 300 MPa. There have also been attempts to produce composites consisting of various amorphous powders [8, 9] fabricated by the consolidation of milled amorphous composite powders. Spark plasma sintering of a highly dense iron-based amorphous alloy reinforced with tungsten particulate composites caused partial devitrification of the amorphous matrix into nanocrystalline  $\text{Fe}_{23}(\text{C,B})_6$ , however, the composites were successfully fabricated. Other possible hardening phases used in aluminum composites are amorphous alloys known for their high strength attaining 1400 MPa by hot compaction of gas-atomized amorphous  $\text{Al}_{85}\text{Ni}_{5}\text{Y}_{8}\text{Co}_2$  powder [11]. Mechanically alloyed amorphous  $\text{Al}_{80}\text{Ni}_{10}\text{Ti}_{10}$  powders mixed with elemental Al were successfully consolidated into composite sheets by cold compaction and rolling. Moreover, the hardness of these composite sheets showed significant improvement with a 5–20 wt.% amorphous  $\text{Al}_{80}\text{Ni}_{10}\text{Ti}_{10}$  phase in the composite [12].

In the present paper, amorphous powder obtained by ball milling was applied to obtain composites based on nanocrystalline silver suitable as contact materials. They are usually well-known silver graphite, silver-nickel, and silver-metal oxide materials [13–19]. The metal oxide used is often cadmium oxide (CdO), but because of its toxicity, it should be replaced by other materials [15]. Therefore in the present paper, the ball-milled amorphous phase obtained from powder mixtures of good glass forming ability [20] was used as a strengthening addition due to its high strength and elastic limit [20]. The other type of composite was the 7475 aluminum alloy base composite strengthened with a low density aluminum based amorphous phase in order to obtain a light alloy composite with a high strength and high elastic limit particles.

## EXPERIMENTAL PROCEDURE

### Materials

Two types of materials were investigated; the first one consisted of silver with additions of 20 wt. % of tungsten and the second one consisted of 20% of an amorphous alloy based on a zirconium quaternary near the eutectic - quaternary composition  $\text{Zr}_{48.5}\text{Cu}_{32}\text{Ti}_{10}\text{Ni}_9$  (Zr1) and the other one based on nickel  $\text{Ni}_{48}\text{Ti}_{20}\text{Nb}_{15}\text{Zr}_{15}$  (Ni1) (numbers indicate at. %). A ball milling process of the alloys was performed in a planetary mill "Pulverisette 5" at 200 rpm in argon atmosphere using bearing steel balls. High purity elemental powders ( $\geq 99.7\%$ ) were handled in a glove box under a purified argon atmosphere. 15 min. of milling was followed by a 45 min. pause for cooling down to avoid overheating of the powders. The elemen-

tal powders were initially blended to the required compositions and then subjected to ball milling. The composites were obtained by hot pressing in vacuum of ball-milled powder mixtures composed either of a 40-hour ball-milled mixture of silver and tungsten in the amount of 20 or 40% or of amorphous powder obtained by 40 hours of ball milling of the earlier mentioned composition -  $\text{Zr}_{48.5}\text{Cu}_{32}\text{Ni}_9\text{Ti}_{10}$  and 20% or 50% of silver powder, previously ball milled for 40 hours to obtain a nanocrystalline structure. The compacting of discs of a 20 mm diameter was performed under vacuum of  $10^{-2}$  bar at a pressure of 600 MPa and temperatures several degrees below the crystallization temperature.

The powder from the 7475 aluminum alloy enriched with zirconium of the composition 5.7% Zn, 2.2% Mg, 0.7% Fe, 1.6% Cu, 0.1% Mn, 0.5% Zr, the rest Al, was obtained from the Norwegian Company. The powders were ball milled for 20 hours to nanocrystallize them and then mixed with an amorphous powder (1:2 ratio) obtained by ball milling of elemental powders of the composition  $\text{Al}_{70}\text{Ni}_{10}\text{Ti}_{10}\text{Zr}_{10}$  (Al-am). The powder mixture was compacted in a similar way to the other one using uniaxial hot pressure compaction in vacuum at a temperature of 380°C and pressure 600 MPa. The weight loss was measured after 50000 electric switching operations for at voltage of 500 V for mobile and immobile contacts.

### Methods

The structure was studied using TEM and HRTEM (Tecnai G2F20 S-Twin) and thin foils from the powders were obtained by immersion in epoxy and thin slicing using a Leica microtome, while those from the composites interfaces for TEM were obtained using a Gatan dimpler and then an ion beam thinning Leica instrument. X-ray diffraction was obtained using an X-ray diffractometer PHILIPS PW 1840, while scanning electron microscopy was carried out using a Philips XL 30 SEM. Compression tests were performed using an Instron 3382 tensile machine using samples of a thickness of 7 mm and diameter 5 mm. Microhardness tests were performed using a CSM-Instruments tester. Thermal effects were studied using a Du-Pont Q910 thermal analyser at the heating rate of 10 K/min.

## RESULTS AND DISCUSSION

Figure 1 shows the X-ray diffraction curves from the milled powders  $\text{Al}_{70}\text{Zr}_{10}\text{Ti}_{10}\text{Ni}_{10}$ ,  $\text{Zr}_{48.5}\text{Cu}_{32}\text{Ti}_{10}\text{Ni}_9$  and  $\text{Ni}_{48}\text{Ti}_{20}\text{Nb}_{15}\text{Zr}_{15}$ . One can see that all the alloys amorphized almost completely, which results from the presence of the broad amorphous halo, however, small peaks are visibly identified as intermetallic compounds formed during milling. The amorphization of all these powders occurred after a milling time from 40–60 hours.

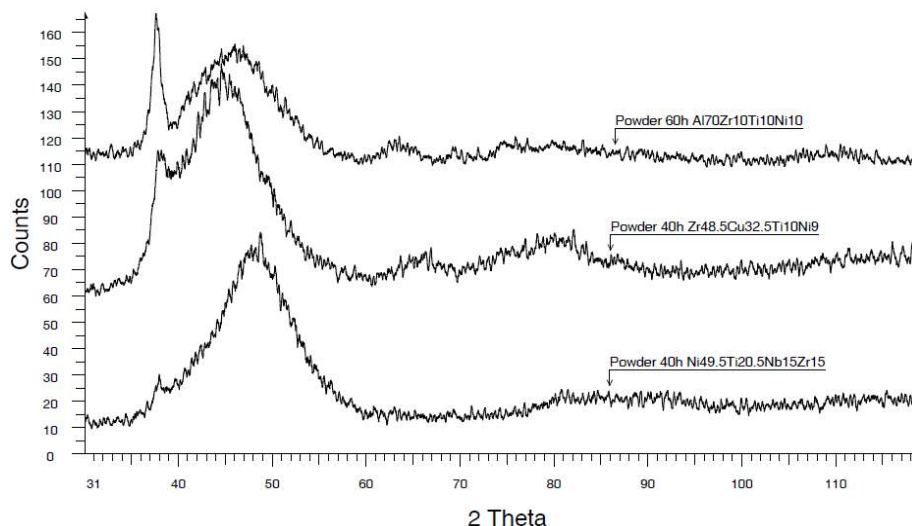


Fig. 1. X-ray diffraction curves from milled powders Al70Zr10Ti10Ni10 for 60 hours (top), Zr48.5Cu32Ti10Ni9 (Zr1) milled 40 h (middle) and Ni48,5Ti20,5Nb15Zr15 milled 40 h (bottom)

Rys. 1. Wyniki badań metodą dyfrakcji rentgenowskiej uzyskane dla mielonych 60 h proszków Al70Zr10Ti10Ni10 (górną), Zr48.5Cu32Ti10Ni9 mielonych 40 h (środek) i Ni48,5Ti20,5Nb15Zr15 mielonych 40 h (dół)

Aluminium base glass forming alloys like AlNiTi [21] are more difficult to amorphize by means of ball milling, than Ni or Zr based ones [20], therefore longer milling times were applied. Amorphization was confirmed by DSC studies, shown in Figure 2, for the alloy Ni48,5Ti20,5Nb15Zr15. One can see that the exothermal crystallization peaks from the rapidly quenched ribbon and the milled powder are slightly different, while the powder has only one peak at higher temperatures. It is most probably caused by the existence of small intermetallic inclusions acting as nuclei for crystallization in the milled powder. They can be seen in the TEM micrographs in Figure 3 in the dark contrast in the bright field and the bright contrast in the dark field, which suggests a different crystal structure there. They were identified as intermetallic phases using a high resolution transmission electron microscopy. The powder particles were mixed with a 40-hour milled silver powder to form composites.

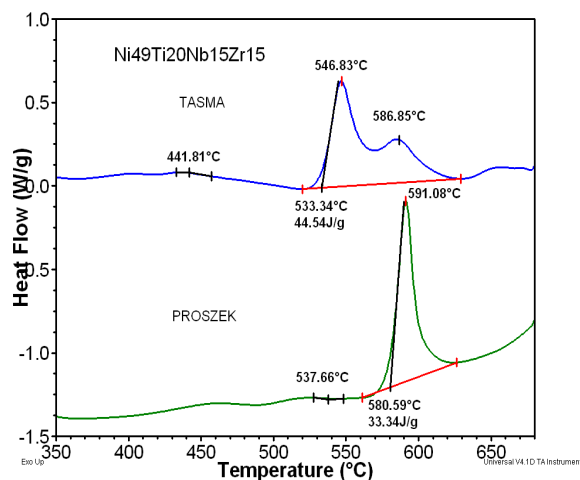


Fig. 2. DSC curves from 40 h milled powder and ribbon from alloy Ni48,5Ti20,5Nb15Zr15 (Ni1)

Rys. 2. Krzywe DSC mielonego 40 h proszku i taśm stopu Ni48,5Ti20,5Nb15Zr15 (Ni1)

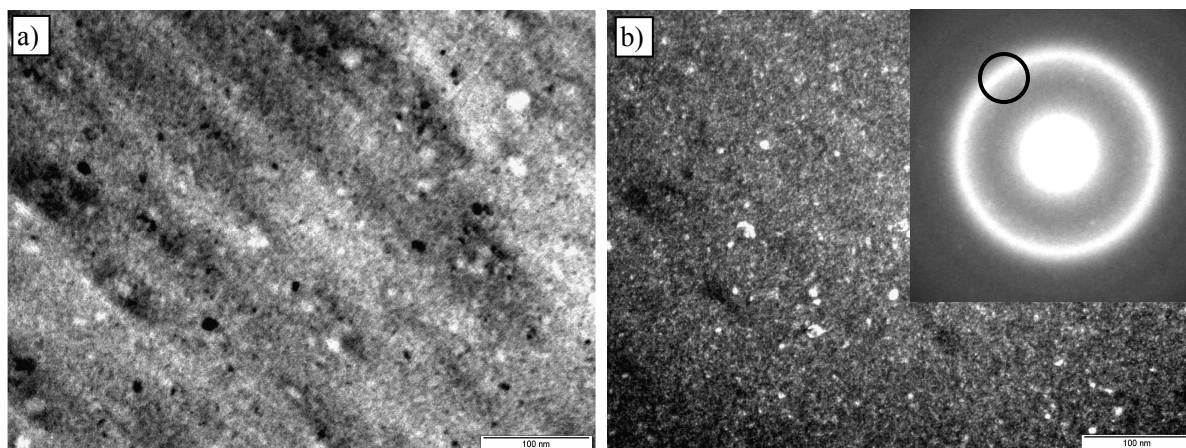


Fig. 3. TEM microstructures from ball-milled Ni1 powders in bright (a) and dark field (b) obtained using fragment of diffused ring marked in SADP as insert from 40-hour milled powder from the alloy

Rys. 3. Mikrostruktury TEM z mielonego proszku Ni1 uzyskane w jasnym (a) i ciemnym polu (b) otrzymane z użyciem fragmentu rozmytego refleksu zaznaczonego na dyfrakcji elektronicznej umieszczonej w rogu (b)

The TEM microstructures of the 40-hour milled silver powder in the bright and dark field, with a Selected Area Diffraction Pattern (SADP) as an insert are shown in Figure 4. One can see that the grain size within the powder particles decreased after milling down to  $50\div 100$  nm. The shape of the grains, with well-developed grain boundaries suggests partial recrystallization of the grains of silver powder. The amorphous powders based on ball-milled Zr1 and Ni1 alloys and nanocrystalline silver powder were mixed together and hot pressed in vacuum.

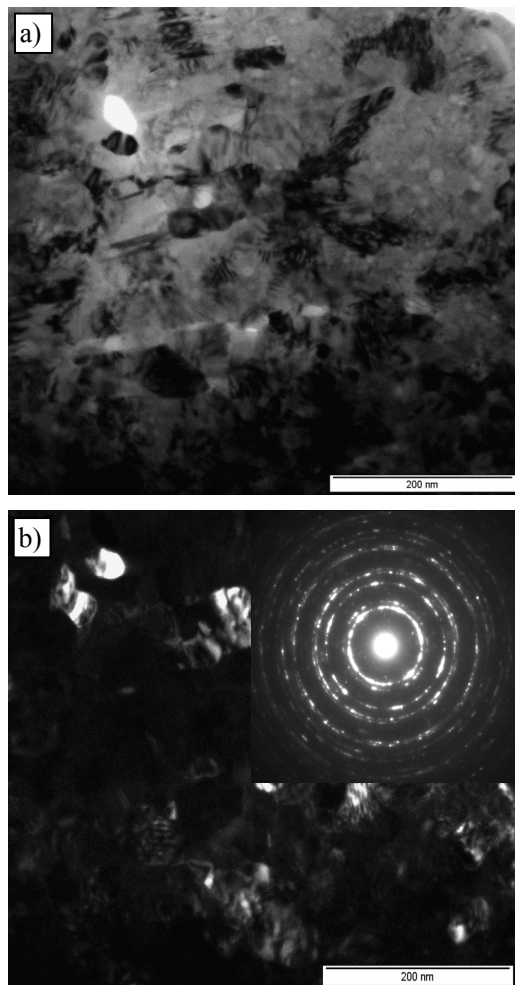


Fig. 4. TEM microstructures from 40-hour ball-milled silver powder obtained in bright (a) and dark field (b). SADP is shown as insert in (b)

Rys. 4. Mikrostruktury TEM z mielonego 40 h proszku srebra uzyskane w jasnym (a) i ciemnym polu (b). Dyfrakcja elektronowa z obszaru na rys. 4 umieszczona w rogu (b)

Figure 5 shows SEM micrographs from compacted composite samples containing 20 wt. % of the amorphous phase Zr1. They show a low porosity and uniform distribution of amorphous particles in the silver matrix. Some amorphous particles show cracks formed during hot pressing resulting most probably from the brittleness of the amorphous phase due to the presence of intermetallic phase particles. No transition layer between the silver grains and the amorphous phase can

be seen at the interfaces at this magnification. The microstructures of composites containing both amorphous additions are similar, therefore only those with a Zr1 amorphous phase addition are presented.

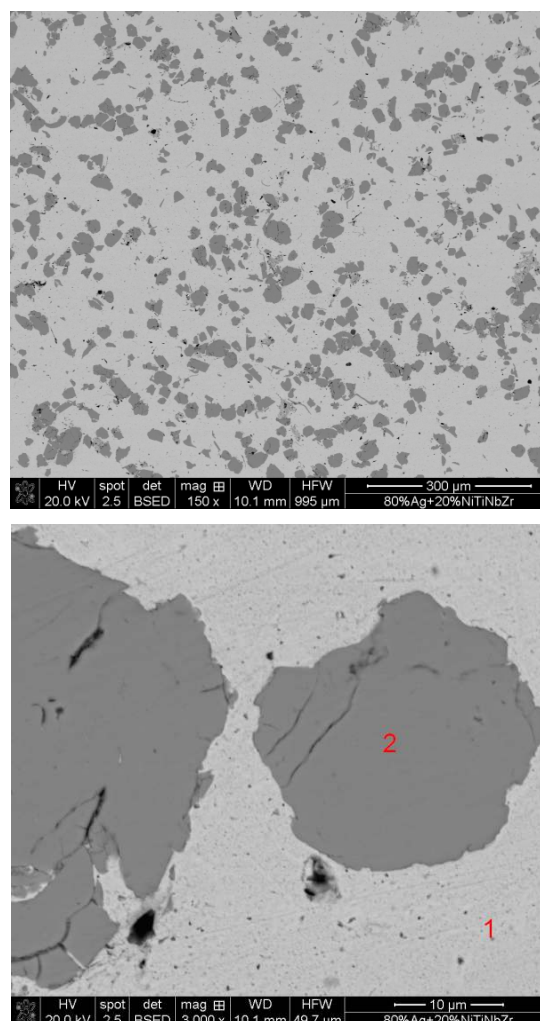


Fig. 5. SEM microstructures from composite 80% Ag+20% amorphous Zr1 powder ball-milled separately for 40 h, then mixed together and hot pressed in vacuum

Rys. 5. Mikrostruktury SEM uzyskane z kompozytu 80% Ag+20% amorficznego Zr1 uzyskanego przez 40 h mielenia w młynkach kulowych, następnie prasowanych na gorąco w próżni

Figure 6 shows a diagram presenting the dependence of the loss of mass of the composite 80%Ag+20%Ni<sub>48,5</sub>Ti<sub>20,5</sub>Nb<sub>15</sub>Zr<sub>15</sub> as a function of the number of current switching operations. The results are different for mobile and immobile switches and the loss of mass is only slightly higher than that obtained for the new composite - Ag-20W [18]. The compression curves of both composites are presented in Figure 7. One can see that the compression strength of both composites is similar, between 250÷300 MPa i.e. lower than that reported for amorphous base composites with 20% Ag [13]. However, the presently investigated composites show a better plasticity of about 2%, which indicates a positive effect of a higher amount of nanocrystalline silver matrix on the plasticity of composites.

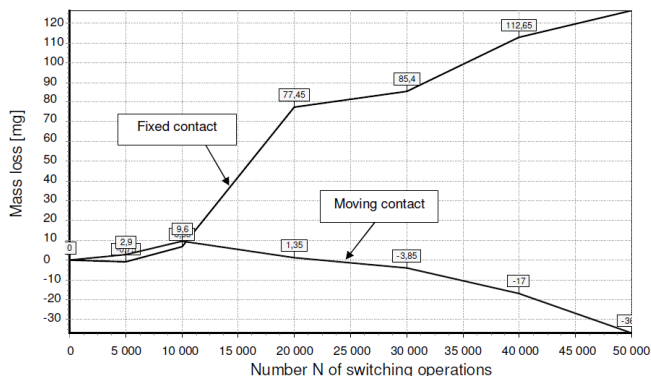


Fig. 6. Diagram showing loss of mass  $\Delta m$  of composite containing 80%Ag+20% amorphous phase Ni<sub>48,5</sub>Ti<sub>20,5</sub>Nb<sub>15</sub>Zr<sub>15</sub> (NiI) as function of number of current switching operations

Rys. 6. Wykres zależności utraty masy kompozytu 80%Ag+20% amorficznej fazy Ni<sub>48,5</sub>Ti<sub>20,5</sub>Nb<sub>15</sub>Zr<sub>15</sub> (NiI) w zależności od ilości N cykli wyłączeniowych

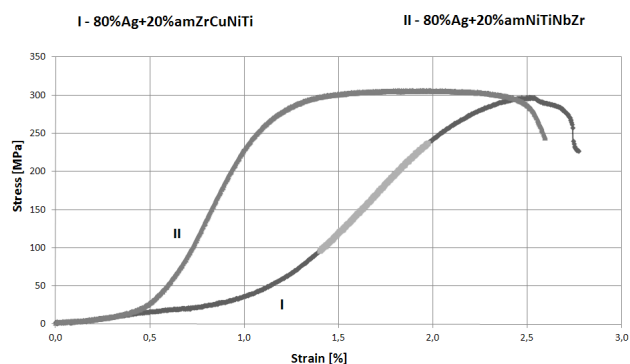


Fig. 7. Compression curves of composites with additions of Zr<sub>48,5</sub>Cu<sub>32</sub>Ti<sub>10</sub>Ni<sub>9</sub> and Ni<sub>48,5</sub>Ti<sub>20,5</sub>Nb<sub>15</sub>Zr<sub>15</sub>

Rys. 7. Krzywe z próby ściskania kompozytów z dodatkami 20% Zr<sub>48,5</sub>Cu<sub>32</sub>Ti<sub>10</sub>Ni<sub>9</sub> lub Ni<sub>48,5</sub>Ti<sub>20,5</sub>Nb<sub>15</sub>Zr<sub>15</sub>

Another type of composites with the participation of the amorphous phase investigated in the present paper is based on the milled amorphous alloy Al<sub>70</sub>Ni<sub>10</sub>Zr<sub>10</sub>Ti<sub>10</sub> with the addition of 34 wt.% of the nanocrystalline ball-milled prealloyed 7475 alloy to improve plasticity, using a similar concept as in composites with copper additions [8, 9]. It can be explained by the nucleation of cracks within the amorphous similar to that in [4] where 40% of a crystalline phase was added. The TEM microstructure in Figure 8 shows the amorphous 7475 alloy interface, where one can see no intermediate layer at the interface. The growth of grains up to 400 nm occurred due to the small amount of grain growth controlling elements. The darker, smaller particles are the intermetallic phases like MgZn<sub>2</sub> grown during hot pressing.

The average microhardness of the amorphous phase within the composites is 670 HV, while that of the 7475 alloy is only 200 HV. In view of such hardness values, the compression strength of 420 MPa resulting from the stress/strain curve in Figure 9a seems to be rather low, however, similar to that obtained by those with copper additions [8, 9]. It can be explained by the nucleation and propagation of cracks within the amorphous phase, which can be seen in the SEM micrograph in Figure 9b

of a sample deformed in the compression test. Easy cracking of the amorphous phase is most probably caused by a large fraction of intermetallic particles within the amorphous component (which can be seen in TEM micrograph and electron diffraction pattern in Fig. 8) and therefore a low toughness of the composite.

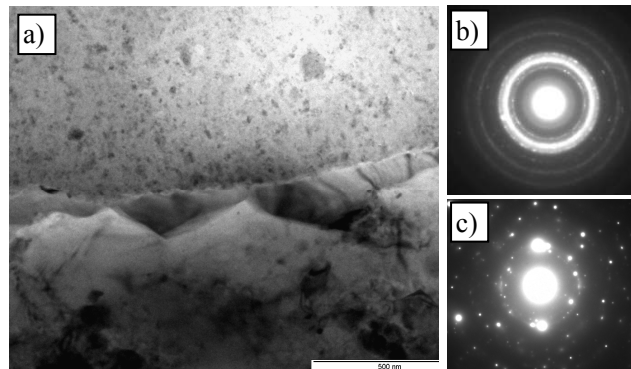


Fig. 8. Composite of 66% of amorphous phase and 7475 alloy (a) TEM micrograph from interface, (b) SADP from upper partially amorphous part (c) SADP from central lower part of 7475 alloy

Rys. 8. Kompozyt zawierający 66% fazy amorficznej wzmacniającej i stopu aluminium 7475. (a) Mikrostruktura TEM granicy międzyfazowej. (b) Dyfrakcja elektronowa z centralnej części fazy częściowo amorficznej. (c) Dyfrakcja z centralnego obszaru stopu 7475 widoczny w dolnej części mikrostruktury

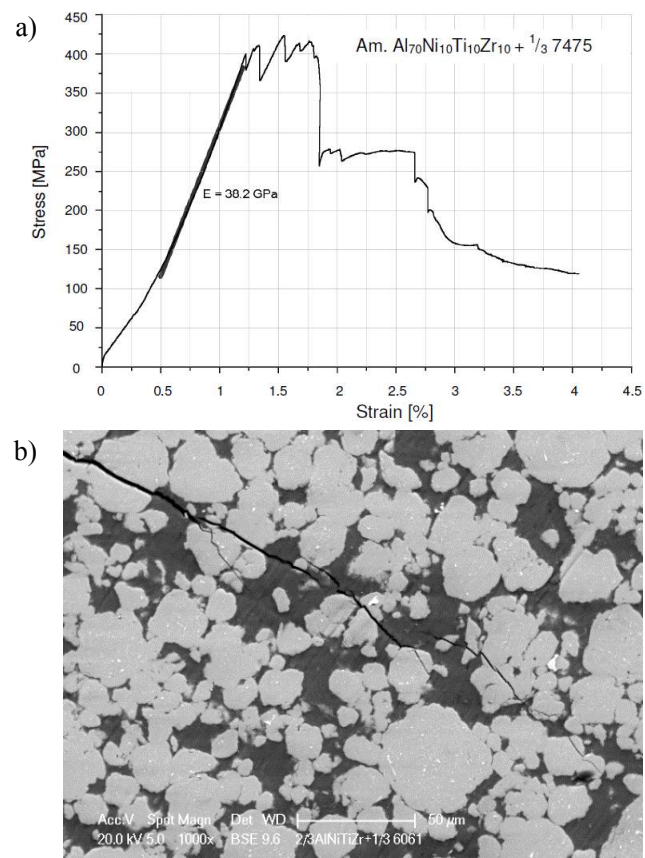


Fig. 9. Compression curve of composite containing 66% of aluminum base amorphous phase and 34% of milled 7475 alloy (a) and SEM microstructure of compression deformed sample (b)

Rys. 9. Krzywa ściskania kompozytu zawierającego 66% fazy amorficznej na osnowie aluminium i 34% stopu 7475 (a). Mikrostruktura SEM próbki odkształconej w próbie ściskania (b)

## CONCLUSIONS

1. The nanocrystalline silver base composites with the addition of 20% of the amorphous phases obtained using ball milling, based either on zirconium or nickel possess better mechanical properties (near 300 MPa) than the recently elaborated contact materials - Ag-W. They also show similar weight loss during 50000 voltage switching operations.
2. The composites containing 2/3 of the amorphous phase based on aluminum of the composition Al70Ni10Zr10Ti10 obtained using ball milling mixed with nanocrystalline 7475 alloy powder, show a rather low compression strength of 420 MPa due to crack nucleation within the amorphous phase, which cannot be prevented by the 34% of fine crystalline 7475 alloy addition, which has shown excessive grain growth up to 0.4  $\mu\text{m}$ .

## Acknowledgements

*The financial support from the research grant 2011/01/M/ST8/07828 is gratefully acknowledged.*

## REFERENCES

- [1] Jae-Chul Lee, Yu-Chan Kim, Jae-Pyoung Ahn, Hyoung Seop Kim, Acta Materialia 2005, 53, 129-139.
- [2] Taek-Soo Kim, Jae-Young Ryu, Jin-Kyu Lee, Jung-Chan Bae, Materials Science and Engineering A 2007, 449-451, 804-808.
- [3] Lee M.H., Park J.S., Kim J.-H., Kim W.T., Kim D.H., Materials Letters 2005, 59, 1042-1045.
- [4] Chang Kyu Kim, Sunghak Lee, Seung Yong Shin, Do Hyang Kim, Mater. Sci Eng. A, 2007, 449-451, 924-928.
- [5] Chang-Young Son, Chang Kyu Kim, Seung Yong Shin, Sunghak Lee, Mater. Sci. Eng. A 2009, 508, 15-22.
- [6] Huh M.Y., Park E.S., Kim H.J., Bae J.C., Mater. Sci. Eng. A 2007, 449-451, 916-919.
- [7] Lee J.H., Park E.S., Lee J.C., Huh M.Y., Kim H.J., Bae J.C., J. Alloys Comp. 2009, 483, 165-167.
- [8] Lee J.K., Lee M.H., Kim K.B., Intermetallics 2010, 18, 2019-2023.
- [9] Lee J.K., Kim K.B., Lee M.H., Kim T.S., Bae J.C., J. Alloys Comp. 2009, 483, 286-288.
- [10] Ashish Singh, Sandip P. Harimkar, J. Alloys Compd. 2010, 497, 121-126.
- [11] Kawamura Y., Mano H., Inoue A., Scripta Mater. 2001, 44 1599-1604.
- [12] Samanta A., Fecht H.-J., Mannac I., Chattopadhyay P.P., Materials Chemistry and Physics 2007, 104, 434-438.
- [13] Dutkiewicz J., Maziarz W., Lityńska-Dobrzyńska L., Rogal Ł., Kanciruk A., Kovačova A., Kompozyty 2008, 8, 220-224.
- [14] Keil A., Werkstoffe fuer elektrische Kontakte, Expert Verlag GmbH, Wuertt 1984.
- [15] Wojtasik K., Missol W., Met. Powder Rep. 2004, 59, 34.
- [16] Findik F., Uzun H., Mater. Des. 2003, 24, 489.
- [17] Slade P.G., IEEE Trans. Comp. Hybrids Manuf. Technol. 1986, 9, 3.
- [18] Aslanoglu Z., Karakas Y., Ovecoglu M.L., Int. J. Powder Metal. 2000, 36, 35.
- [19] Dutkiewicz J., Maziarz W., Lityńska-Dobrzyńska L., Rogal Ł., Góral A., Bidulska J., Kovacova A., Chemicke listy 2011, 105, 420-423.
- [20] C. Suryanarayana, A. Inoue, Bulk Metallic Glasses, CRC Press, Boca Baton, USA, 2011.
- [21] Samanta A., Fecht H.-J., Manna I., Chattopadhyay P.P., Materials Chemistry and Physics 2007, 104, 434-438.
- [22] Dutkiewicz J., Lityńska-Dobrzyńska L., Berent K., Woch M., Osadnik M., Solid State Phenomena, Trans Tech Publications, Proceedings EM2011, accepted for press.